WCTE 2020
WORLD CONFERENCE ON TIMBER ENGINEERING
SANTIAGO, CHILE | 24 - 27 AUGUST

COMPUTATIONAL MECHANICS CONCEPTS FOR WOOD-BASED PRODUCTS AND TIMBER STRUCTURAL ELEMENTS

Markus Lukacevic[1], Josef Füssl[1], Sebastian Pech[1], Christoffer Vida[1], Josef Eberhardsteiner[1]

ABSTRACT: The mechanical behavior of wood products highly depends on structural features on several length scales. This leads to a high amount of random fluctuation in mechanical properties at the structural level. In practice, homogeneous material behavior within timber elements is assumed and uncertainties in loading and load-bearing capacity are considered by using partial safety factors. Those are not directly linked to the mechanical behavior of the considered elements. Therefore, a stochastic framework opening up the possibility to establish such links by combining structural analysis and probabilistic descriptions of wood could be an important step in timber design.

For example, in GLT beams the mechanical behavior mostly depends on the tensile properties of individual boards. To describe their fluctuations, simulations on this level are performed. The reconstruction of knots and the implementation of new fracture mechanical methods allows the prediction of stiffness and strength properties for knot sections. Condensation of those results into stiffness and strength profiles permits the development of probabilistic models and the random generation of such profiles, and their use in wood product simulations. This can be used for sensitivity analyses of timber engineering designs or to obtain probabilistic descriptions of the uncertainties at the level of timber elements.

KEYWORDS: stiffness, strength, fracture mechanics, probabilistic description, sensitivity analysis

1 INTRODUCTION

The future competitiveness of wood compared to other building materials also depends on the development of sophisticated simulation tools. Here, one of the main challenges encountered is the prediction of load bearing capacities based on realistic failure mechanisms. The development of new or the optimization of existing wood-based products and the combined use of wood with other materials requires the description of mechanical processes and their fluctuations in wood. A multiscale modeling approach, starting with the development of a failure criterion for clear-wood [1-3], based on simulations of lower length scales down to the single cell level, its application to realistically modeled wooden boards with knots and fiber deviations [4-5] and the resulting condensation of computationally obtained effective material properties, can be used to transfer information of such varying material properties, and, thus, of uncertainties on several levels, to the timber structural element level [6-7]. Thus, we first present an approach to simulate the fracture behavior of knot sections, which in future will be used to obtain effective strength values of such sections. Then, we show how the results of such simulations can be condensed into so-called stiffness and strength profiles, which next can be used in the simulation of wood products. Here we extend previous modeling approaches for GLT beams [8-13], where such beams were subdivided into sections with assigned material properties. The latest of these models used constant fracture energies for knot sections [14] and employed the extended finite element method (XFEM) [15]. In contrast, in our contribution, we first reconstruct real experiments by virtually reconstructing the lamellas with all knots, which allows us to compare each simulated beam with the experimentally tested one. In addition, the inclusion of cohesive surfaces between the individual lamellas will lead to more realistic global failure mechanisms.

2 FRACTURE SIMULATIONS OF KNOT SECTIONS

Especially for materials with a complex micro- and macro-structure, like wood, crack initiation and propagation are subject to multiple interlinked effects. In wood, crack growth starts on the microscopic level from defects in the cell walls [16]. As those cracks localize – close to reaching the peak load – the actual macro crack opens. After crack initiation so-called fiber bridging

[1] Markus Lukacevic, Vienna University of Technology (TU Wien), Austria, markus.lukacevic@tuwien.ac.at
Josef Füssl, Vienna University of Technology (TU Wien), Austria, josef.fuessl@tuwien.ac.at
Sebastian Pech, Vienna University of Technology (TU Wien), Austria, sebastian.pech@tuwien.ac.at
Christoffer Vida, Vienna University of Technology (TU Wien), Austria, christoffer.vida@tuwien.ac.at
Josef Eberhardsteiner, Vienna University of Technology (TU Wien), Austria, josef.eberhardsteiner@tuwien.ac.at

causes toughening effects that result in a cohesive facture behavior [17].

In order to properly model such cracks, the recently emerging phase field method for fracture offers an implicit geometric representation of a crack, which, in theory, allows topologies of arbitrary complexity [18-19]. The original theory is limited to brittle fracture of isotropic materials. However, in recent years, implementations regarding extensions towards

- plastic behavior, based on cohesive zone models [20],
- anisotropic constitutive laws [21] and
- anisotropic fracture energy release rates [22-23]

were proposed.

In the phase field method, a sharp crack Γ_c in a body Ω is approximated by a diffusive crack zone $\Gamma_c(d)$ where d is the so-called phase field variable. $d \in [0,1]$ defines the crack topology, with $d = 0$ as the uncracked state and $d = 1$ as the fully cracked state. The width of the transition zone is characterized by a regularization parameter, the so-called length scale parameter.

The entire theory is built around a variational model of Griffith's theory that is put into an energy minimization scheme of the total energy of the system (excluding contributions of body and surface loads here):

$$\Pi = \int_\Omega \left[\omega(\boldsymbol{d})\, \psi^+(\boldsymbol{\varepsilon}) + \psi^-(\boldsymbol{\varepsilon})\right] dV + \sum_{i=1}^{n} G_{c,i} \int_\Omega \gamma_i(d_i, \nabla d_i, \boldsymbol{A}_i)\, dV,$$

where $\boldsymbol{d}$ is a vector of phase field variables of length n, ω is the degradation function that damages the solid, ψ^+ is the fracture contributing or active part of the strain energy density, ψ^- is the inactive or passive part of the strain energy density, $G_{c,i}$ is the fracture energy release rate of the i-th phase field variable, $\boldsymbol{A}_i$ is a second order tensor, the so-called structural tensor, defining the anisotropic properties in form of preferable crack directions or weak fracture planes, and γ_i is the crack surface density which approximates the sharp crack as a volume integral:

$$\Gamma_{c,i} \approx \Gamma_{c,i}(d_i) = \int_\Omega \gamma_i(d_i, \nabla d_i, \boldsymbol{A}_i) dV$$

For modeling the anisotropic behavior of wood, two different approaches are applied in this work: To distinguish different failure mechanisms, two phase field variables are used, one for the longitudinal (L) direction and one for the radial-tangential (RT) plane. Additionally, the structural tensor is used to scale the phase field's gradient in the RT plane such that the L direction is favorable for crack propagation.

This coupled FEM problem is solved using a so-called staggered approach. Here, first, the deformation field is fixed and the phase field sub-problem is solved. Subsequently, the phase field variables are fixed, and the deformation problem is solved using the newly obtained phase field variables.

The model is first tested with a simple single edge notch tension test, where the fiber inclination is varied from 0° to 90° (see Figure 1). The test clearly shows that the expected behavior of having a crack opening along the weak axis of the material can be modeled. At the point where stresses in L direction dominate, the failure mode switches and a crack opens perpendicular to the fiber direction.

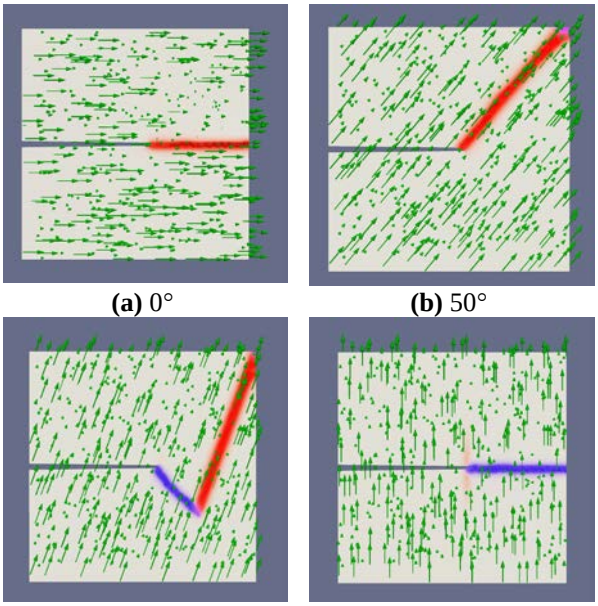

(a) 0° **(b)** 50° **(c)** 70° **(d)** 90°

Figure 1*: Single edge notch plates tested for various fiber angles. The fiber direction is depicted by green arrows. The plates are held both at top and bottom and are loaded in form of a prescribed vertical deformation at the top edge. The phase field variables are depicted in blue for the L direction and red for the RT plane.*

By implementing this new approach into previous developments of a numerical simulation tool for wooden boards [4-6], which is able to consider morphological features at the single board level, like virtually reconstructed knot inclusions and fiber deviations in their vicinities, realistic simulations of complex failure mechanisms of not only single wooden boards and their use in timber connections but also of more complex wood-based products, like Glulam and CLT elements, are rendered possible.

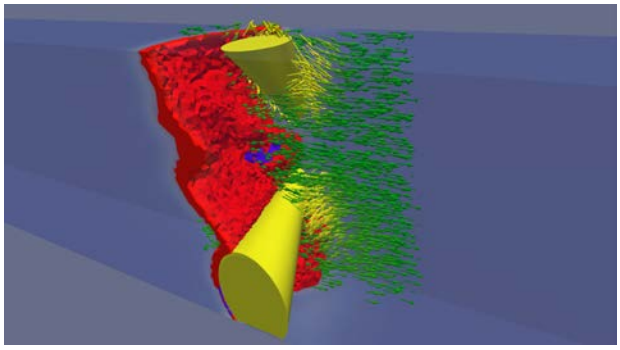

Figure 2: *Crack between two knots. The blue region depicts crack phase field* $\boldsymbol{d_1 > 0.95}$*, the red region crack phase field* $\boldsymbol{d_2 > 0.95}$*. The green and yellow arrows depict the fiber directions, where the more yellow an arrow is, the more it deviates from the beam's longitudinal axis.*

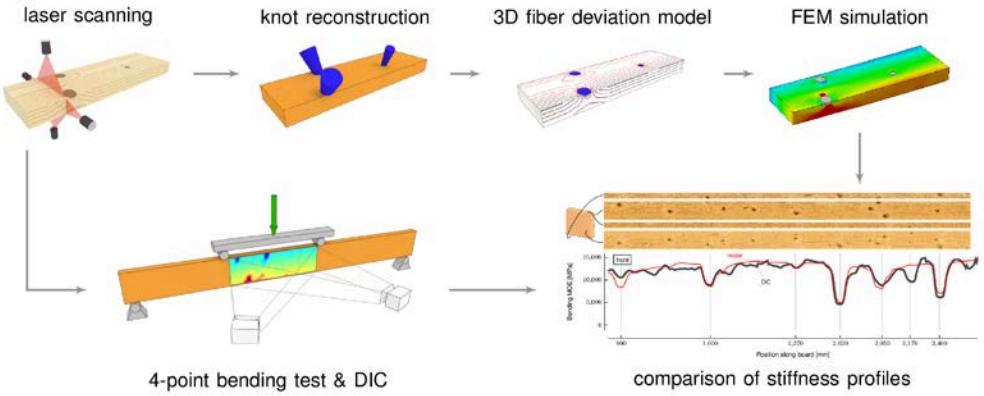

Figure 3: *Modeling approach for obtaining effective material properties based on commonly used laser scanning of timber boards during the strength grading process [5]*

In order to gain insight into the capabilities of the model being able to compute complex crack geometries, a tensile test of a specimen including two knots was performed (see Figure 2). The crack initiation starts at the lower knot in a region that is highly stressed perpendicular to the fiber and then propagates upwards. Obviously, by geometrically describing cracks as a continuous field, it is possible to model very complex crack topologies.

3 DERIVATION OF EFFECTIVE MATERIAL PROPERTY PROFILES

The detailed simulation of entire timber structures including all their local defects, like knots, up to the point of failure is most likely not feasible. However, by being able to compute the failure mechanisms of arbitrary sections of wooden boards, it is possible to consider the spatial variability and uncertainty of mechanical properties, in particular stiffness and strength, of single boards with effective material profiles.

An example of such a condensed effective material profile is shown in the following [5]. Here, bending stiffness profiles are compared for a board subjected to four-point bending. For the experimental profile, a strain field on the board surface was computed by using digital image correlation measurements and by estimating the local cross sectional bending stiffness of the board with linear fits into the strain fields (see Figure 3 for the modeling approach). For the numerical simulations, the virtually reconstructed board with computed fiber deviations was subjected to the same boundary conditions in an elastic FEM simulation. The comparison of a sample board in Figure 4 shows the capabilities of our well-validated numerical simulation tool to capture even local stiffness effects accurately.

For the simulation of GLT beams in the next section, this approach is now simplified even further. Instead of continuous stiffness profiles, we now introduce piecewise constant ones, according to a previous subdivision of

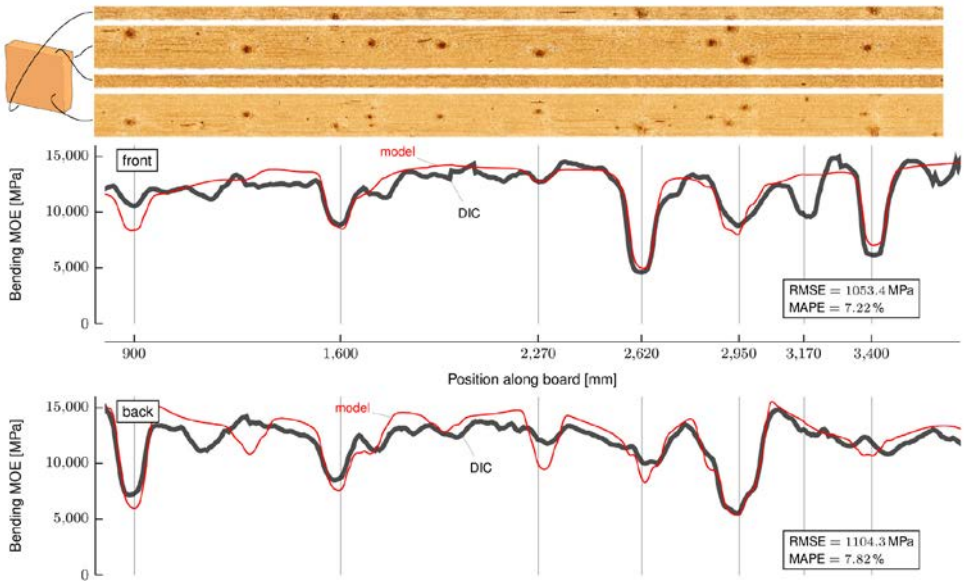

Figure 4: *Comparison of experimentally and numerically obtained bending stiffness profiles [5]*

individual lamellas into knot and clear wood sections. The abovementioned simulations were performed not just for a single board section but for all previously defined sections of a lamella (see Figure 5). The obtained results can be evaluated and processed into piecewise constant stiffness and strength profiles. For the latter ones, previously determined indicating properties (IPs) for knot groups under longitudinal tension [24] were used instead of fracture mechanics simulations. As for other wood product types additional effective strength properties might be of interest, the same workflow could also be applied, e.g. for shear or perpendicular-to-grain virtual loading conditions.

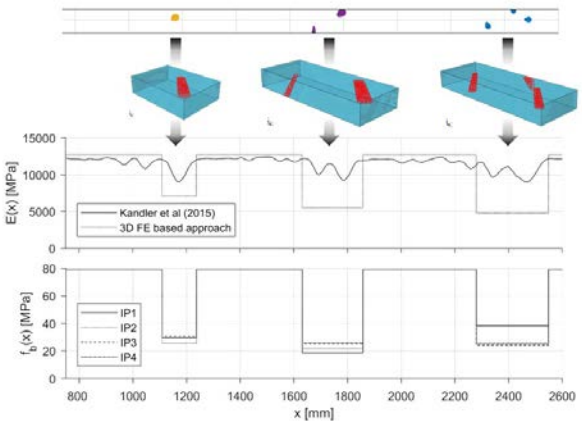

Figure 5: *During the virtual reconstruction process, knots are grouped into so-called knot sections, for which FE models are generated. The corresponding simulation results information is then condensed into stiffness and strength profiles.*

4 SIMULATION OF WOOD PRODUCTS

The previously obtained profiles of piecewise constant and effective material properties are now assigned to GLT beams, where the positions of the scanned and virtually reconstructed lamellas are known. This allows for the direct comparison of numerical and experimental results, with respect to the beams' load-bearing behavior, i.e. global bending strength and failure mechanisms.

The GLT beam model (see Figure 6) is subjected to a four-point bending test, where discrete cracks in timber boards by means of XFEM and delamination between lamellas using cohesive surface properties are considered. For the former a modified traction-separation law is used, where the strength value is assigned to the section according to the corresponding strength profile of the lamella and constant fracture energies ($G = 20.0\ \mathrm{Nmm/mm^2}$) are used. For the simulation of the quasi-delamination effect, which allows vertical cracks to "jump" to another location, both constant strength ($f_n = 100.0\ \mathrm{N/mm^2}$ and $f_s = f_t = 10.0\ \mathrm{N/mm^2}$) and fracture energy ($G = 1.0\ \mathrm{Nmm/mm^2}$) properties are assigned. This approach allows the representation of the rather complex failure behavior of GLT beams in a simplified way with restrictions regarding crack directions (only vertical ones in lamellas) and crack initiation. The test series consisted of four different GLT beam setups, with two groups of beam types with four lamellas and two groups of beam types with ten lamellas. In addition, by introducing two different strength classes this leads to a total of four GLT beam types (A/T14-4 = type A with 4 lamellas of strength class T14, B/T22-4, D/T14-10 and E/T22-10). The exact dimensions and the description of the experimental findings can be found in [25]. For the numerical simulations the commercial FE software Abaqus (from Dassault Systèmes, Vélizy-Villacoublay, France) was used and all simulations were performed on a high-performance computer cluster.

4.1 Mesh size study

To determine an efficient FE mesh size with regard to sufficient accuracy and manageable simulation times, we first varied the mesh size by controlling the number of elements in thickness direction per lamella from one to five elements. All other simulation parameters were kept constant. The resulting differences in load bearing capacities can be seen in Figure 7 for all four beam types. For better comparability, the load-bearing capacities were normalized to the simulation result of the finest mesh (five elements per lamella in thickness direction). It can be noticed that except for two outliers, a mesh size of three elements per timber board height is sufficient. In the model of the outlier (marked in Figure 7a) a clear wood lamella was present at the tensile loaded edge. Thus, the models with one or two elements per board thickness cannot capture the high tensile stresses close to the bottom edge and failure occurred in adjacent knot sections. In contrast, the finer meshes led to failure of mentioned clear wood section. The outlier in Figure 7d is caused by the

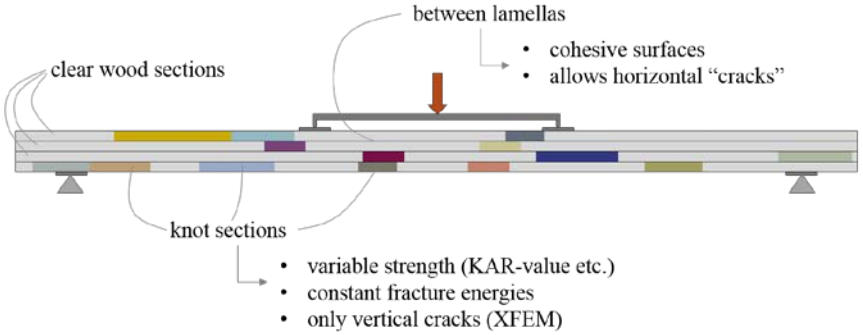

Figure 6: *GLT modeling approach and test setup*

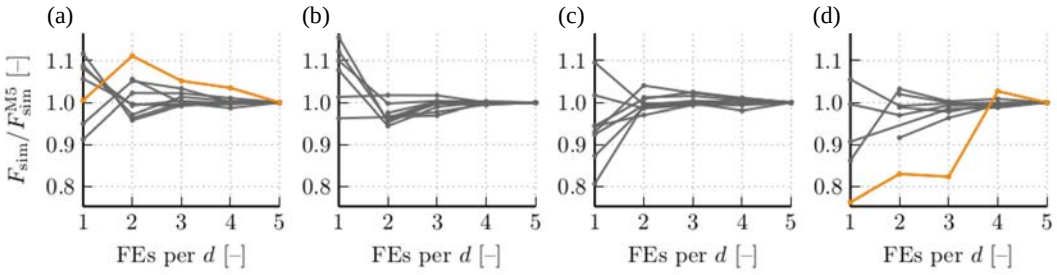

Figure 7: *Dependency of mesh size (number of finite elements per lamella in thickness direction) on the load-bearing capacity F_{sim} , with F_{sim} being normalized to F_{sim} for five elements per lamella in thickness direction, for all four beam types: (a) A/T14-4, (b) B/T22-4, (c) D/T14-10 and (d) E/T22-10. The orange color marks outliers, defined by a difference >4% the results with three elements compared to the ones for five elements. [26]*

inability of the coarse mesh model to correctly capture a load redistribution effect and subsequent load increase, which can be modeled by finer meshes.

4.2 Failure mechanisms

As already mentioned, all GLT beam simulation models are based on real experimental setups with realistic consideration of knot sections. Thus, an emphasis of this work was on the representation of experimentally observed failure mechanisms, which differ for the various beam setups, i.e. number of laminations and strength class, which has been shown in [25]. In that paper, also failure modes were documented in detail.

An exemplary comparison of numerically and experimentally obtained failure mechanisms is shown in Figure 8 for a beam of Type B. Within the higher strength class (T22), a rather small number of knot sections is present in the bottom lamella. Thus, failure starts in the first knot section in the right quarter of the model and then extends towards the beam's left end. For this strength class, very similar mechanisms could also be observed in the experiments.

Another comparison is shown in Figure 9 for a GLT beam of type D (10 laminations and strength class T14). Here, the lower strength class leads to a rather localized and brittle failure mechanism in the region with the highest bending moment. The first three lamellas (from the bottom) fail first in vertical direction, before the cracks extend in horizontal direction. Although the exact location of the initial vertical crack could not be predicted, the general failure mechanisms could be reproduced very well.

4.3 Prediction of load-bearing capacity

Figure 10 shows the model's capability to predict both system stiffness and load-bearing capacity in comparison to the experiments. The system stiffness was evaluated for both simulations and experiments by evaluating the

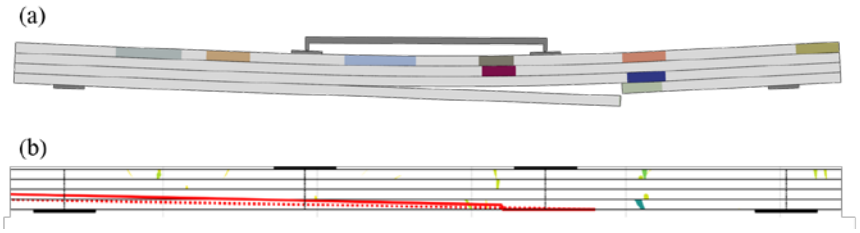

Figure 9: *(a) numerically [26] and (b) experimentally [25] obtained failure mechanisms for a GLT beam of type B (4 laminations, T22)*

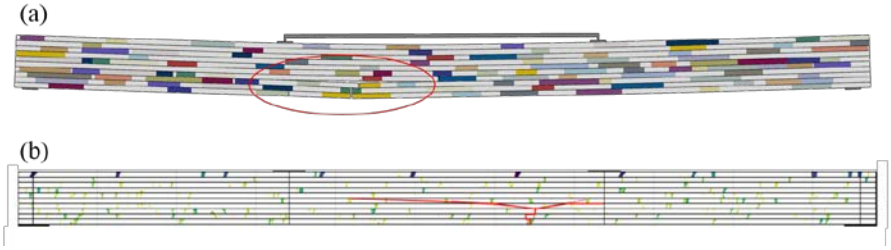

Figure 8: *(a) numerically [26] and (b) experimentally [25] obtained failure mechanisms for a GLT beam of type D (10 laminations, T14)*

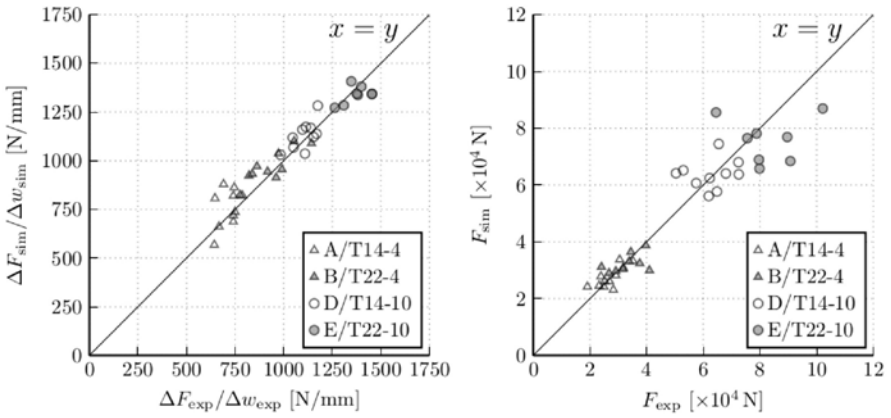

Figure 10: *Simulated versus experimental system stiffness (left) and load-bearing capacity (right) for all tested GLT beams [26]*

stiffness in the load-displacement diagrams linearly between 10 % and 40 % of the maximum load. As can be clearly seen the model approximates the experimental system stiffness very well.

To estimate the GLT load-bearing capacity, the following approach is used to determine the peak load. If the load decreases during the simulation by at least 3 %, the corresponding load before the load drop is defined as the maximum simulation load. In addition, two energy criteria must be fulfilled, which limit the amount of viscous regularization energies to obtain reasonable solutions. As can be seen on the right of Figure 10, the maximum loads can also be predicted well with a coefficient of determination of $R^2 = 0.88$.

5 CONCLUSIONS AND OUTLOOK

Our main research aim is to use this simulation approach in the development of new wood composites by making the material wood more predictable and thus more interesting for engineering applications. As the simulation of larger structures of wood-based products, where all inhomogeneities are modeled in high detail, might be not feasible in the near future, we developed a framework for sensitivity analysis and robust design optimization of structures made out of wood-based products [6,27], which is based on a random material model for both stiffness and strength properties of individual laminations.

By combining detailed simulations on various length scales and condensing this information into so-called stiffness and strength profiles, we are able to also simulate realistic failure mechanisms on the wood product level and to estimate their load-bearing capacities.

Thus, this concept must be consistently improved on several levels, as presented in this paper. The proper estimation of strength properties for knot sections is one of the main focuses of current research efforts. Another important step towards a complete modeling concept for mass timber components is the adequate condensation of the obtained local material properties and their fluctuations into models with lower degrees of detail, but which must still be able to capture all important system effects.

Finally, the validation of such an approach on all levels, like the detailed reconstruction of GLT beams and the comparison to experimentally obtained failure mechanisms, completes our modeling strategy.

Next, by also developing random process models, able to capture the characteristics of the stiffness and strength profiles, also predictions on statistical strength properties of various strength classes can be made. A previous application of such an approach [7] already showed that for CLT plates under concentrated loading the use of such strength profiles led to very good estimates of not only the mean value but also the standard deviations of the bending strength.

In another application [28], stiffness profiles are used in a metamodel assisted optimization of glued laminated timber systems by reordering laminations using metaheuristic algorithms. This allows the optimized assignment of a batch of laminations to a set of GLT beams, such that an optimized load-bearing behavior is achieved.

This framework also can be easily incorporated into existing workflows where specific mechanical models are already established. An additional further development of all individual steps within this framework, e.g. by improving fracture mechanics simulations of knot sections, will lead to improved prediction capabilities and, thus, more efficient timber structures.

ACKNOWLEDGEMENT

This work was supported by the FWF Austrian Science Fund through the START grant Y1093 and the ERA-NET Cofund Action ‘ForestValue’.

REFERENCES

[1] M. Lukacevic, J. Füssl: Application of a multisurface discrete crack model for clear wood taking into account the inherent microstructural characteristics of wood cells. Holzforschung, 70(9):845–853, 2016.

[2] M. Lukacevic, J. Füssl, R. Lampert: Failure mechanisms of clear wood identified at wood cell

level by an approach based on the extended finite element method. Engineering Fracture Mechanics, 144:158–175, 2015.

[3] M. Lukacevic, W. Lederer, J. Füssl: A microstructure-based multisurface failure criterion for the description of brittle and ductile failure mechanisms of clear-wood. Engineering Fracture Mechanics, 176:83-99, 2017.

[4] M. Lukacevic and J. Füssl: Numerical simulation tool for wooden boards with a physically based approach to identify structural failure. European Journal of Wood and Wood Products, 72(4):497–508, 2014.

[5] M. Lukacevic, G. Kandler, M. Hu, A. Olsson, J. Füssl: A 3D model for knots and related fiber deviations in sawn timber for prediction of mechanical properties of boards. Materials & Design, 166:107617, 2019.

[6] G. Kandler, M. Lukacevic, C. Zechmeister, S. Wolff, J. Füssl: Stochastic engineering framework for timber structural elements and its application to glued laminated timber beams. Construction and Building Materials, 190:573–592, 2018.

[7] M. Li, J. Füssl, M. Lukacevic, C.M. Martin, J. Eberhardsteiner: Bending strength predictions of cross-laminated timber plates subjected to concentrated loading using 3D finite-element-based limit analysis approaches. Composite Structures, 220:912–925, 2019.

[8] R. O. Foschi, J. D. Barrett: Glued-laminated beam strength: A model. Journal of the Structural Division, 106(8):1735–1754, 1980.

[9] J Ehlbeck, F Colling, R Görlacher: Einfluß keilgezinkter Lamellen auf die Biegefestigkeit von Brettschichtholzträgern. Holz als Roh-und Werkstoff, 43(8):333-337, 1985.

[10] F. Colling, R.H. Falk: Investigation of laminating effects in glued-laminated timber. CIB-W18/26-12-1, Athens, Georgia, USA, 1993.

[11] H. Blaß, M. Frese, P. Glos, J. Denzler, P. Linenmann, A. Ranta-Maunus: Zuverlässigkeit von Fichten-Brettschichtholz mit modiziertem Aufbau. KIT Scientific Publishing Vol, 11, 2008.

[12] E. Serrano, J. Gustafsson, H.J. Larsen: Modeling of finger-joint failure in glued-laminated timber beams. Journal of Structural Engineering, 127(8):914-921, 2001.

[13] G. Fink: Influence of varying material properties on the load-bearing capacity of glued laminated timber. PhD thesis, ETH Zurich, 2014.

[14] L. Blank, G. Fink, R. Jockwer, A. Frangi: Quasi-brittle fracture and size effect of glued laminated timber beams. European Journal of Wood and Wood Products 75(5):667–681, 2017.

[15] C. T. Camú, S. Aicher: A stochastic finite element model for glulam beams of hardwoods. World Conference on Timber Engineering. Seoul, South Korea, 2018.

[16] I. Smith, E. Landis, and M. Gong, Fracture and fatigue in wood. Chichester, West Sussex, England; Hoboken, NJ: J. Wiley, 2003.

[17] S. Vasic, I. Smith, E. Landis: Fracture zone characterization - Micro-mechanical study. Wood and Fiber Science, 34:42–56, 2002.

[18] C. Miehe, F. Welschinger, M. Hofacker: Thermodynamically consistent phase-field models of fracture: Variational principles and multi-field FE implementations. Int. J. Numer. Methods Eng., 83(10):1273–1311, 2010.

[19] B. Bourdin, G. A. Francfort, J.-J. Marigo: Numerical experiments in revisited brittle fracture. Journal of the Mechanics and Physics of Solids 48(4):797–826, 2000.

[20] J.-Y. Wu, V. P. Nguyen: A length scale insensitive phase-field damage model for brittle fracture. J. Mech. Phys. Solids, 119:20–42, 2018.

[21] N. P. van Dijk, J. J. Espadas-Escalante, P. Isaksson: Strain energy density decompositions in phase-field fracture theories for orthotropy and anisotropy. International Journal of Solids and Structures, 196–197:140–153, 2020.

[22] J. Bleyer, R. Alessi: Phase-field modeling of anisotropic brittle fracture including several damage mechanisms. Comput. Methods Appl. Mech. Eng., 336:213–236, 2018.

[23] S. Teichtmeister, D. Kienle, F. Aldakheel, M.-A. Keip: Phase field modeling of fracture in anisotropic brittle solids. Int. J. Non Linear Mech., 97:1–21, 2017.

[24] M. Lukacevic, J. Füssl, J. Eberhardsteiner: Discussion of common and new indicating properties for the strength grading of wooden boards. Wood Science and Technology, 49(3):551-576, 2015.

[25] G. Kandler, M. Lukacevic, J. Füssl: Experimental study on glued laminated timber beams with well-known knot morphology. European Journal of Wood and Wood Products, 76(5):1435-1452, 2018.

[26] C. Vida: Computational modeling approach for glued laminated timber based on quasi-brittle material behavior and well-known knot morphology. Master's thesis, TU Wien, 2020.

[27] J. Füssl, M. Lukacevic, S. Pillwein, H. Pottmann: Computational Mechanical Modelling of Wood—From Microstructural Characteristics Over Wood-Based Products to Advanced Timber Structures. In: Digital Wood Design (pp. 639-673). Springer, Cham, 2019.

[28] S. Pech, G. Kandler, M. Lukacevic, J. Füssl: Metamodel assisted optimization of glued laminated timber beams by using metaheuristic algorithms. Engineering Applications of Artificial Intelligence, 79:129-141, 2019.